Cerebral Cortex Advance Access published January 29, 2013

Cerebral Cortex
doi:10.1093/cercor/bht006

Functional Magnetic Resonance Imaging Adaptation Reveals the Cortical Networks for Processing Grasp-Relevant Object Properties

Simona Monaco[1,2], Ying Chen[1,2], W. Pieter Medendorp[3], J. Douglas Crawford[1,2,4,5], Katja Fiehler[6] and Denise Y.P. Henriques[1,2,4]

[1]York University, Centre for Vision Research, Toronto, ON, Canada, [2]Canadian Action and Perception Network (CAPnet), [3]Radboud University Nijmegen, Donders Institute for Brain, Cognition and Behaviour, Nijmegen 6500HB, The Netherlands, [4]Departments of Psychology, Kinesiology, Health Sciences, and Neuroscience Graduate Diploma Program, York University, Toronto, ON, Canada, [5]Department of Biology, York University, Toronto, ON, Canada and [6]University of Giessen, Experimental Psychology, Giessen, Germany

Address correspondence to Simona Monaco, York University, Computer Science and Engineering Building, 4700 Keele Street, Toronto, ON, Canada M3J 1P3. Email: simona.monaco@gmail.com

Grasping behaviors require the selection of grasp-relevant object dimensions, independent of overall object size. Previous neuroimaging studies found that the intraparietal cortex processes object size, but it is unknown whether the graspable dimension (i.e., grasp axis between selected points on the object) or the overall size of objects triggers activation in that region. We used functional magnetic resonance imaging adaptation to investigate human brain areas involved in processing the grasp-relevant dimension of real 3-dimensional objects in grasping and viewing tasks. Trials consisted of 2 sequential stimuli in which the object's grasp-relevant dimension, its global size, or both were novel or repeated. We found that calcarine and extrastriate visual areas adapted to object size regardless of the grasp-relevant dimension during viewing tasks. In contrast, the superior parietal occipital cortex (SPOC) and lateral occipital complex of the left hemisphere adapted to the grasp-relevant dimension regardless of object size and task. Finally, the dorsal premotor cortex adapted to the grasp-relevant dimension in grasping, but not in viewing, tasks, suggesting that motor processing was complete at this stage. Taken together, our results provide a complete cortical circuit for progressive transformation of general object properties into grasp-related responses.

Keywords: functional magnetic resonance imaging adaptation, grasping, grasp-relevant dimension, object size

Introduction

The properties of an object are processed not only based on its physical appearance, like the surface and shape, but also on the possible actions that it could afford depending on our motor capabilities (Gibson 1979). For instance, if the intent is to grasp an object, then the graspable dimension becomes the most relevant property (Ganel and Goodale 2003). In fact, planning a precision grip requires the selection of the grasp axis on the object (distance between selected locations for index finger and thumb), which will determine the grip aperture. We will refer to this axis as the graspable or grasp-relevant dimension of an object. Usually, an object has several potential graspable dimensions that depend on general object properties, and that become evident after a quick initial analysis of the object. However, very little is known about the cortical mechanisms that derive the graspable dimension from more general object properties, and the degree to which these processes might be separated at the neural level is not yet understood.

Both primate electrophysiology and human neuroimaging studies have implicated several cortical areas in coding object properties, like size and shape. For example, it has been shown that dorsal stream areas, such as the anterior intraparietal area (AIP), process size, and shape of objects for grasping actions (macaques: Murata et al. 2000; Asher et al. 2007; Gardner et al. 2007; humans: Cavina-Pratesi et al. 2007; Kroliczak et al. 2008; Chouinard et al. 2009; Monaco et al. 2010). In addition, an area in the superior parietal occipital cortex of humans (SPOC) and macaques (V6A) is involved in processing and coordinating several components of grasping actions (humans: Cavina-Pratesi et al. 2010; Gallivan et al. 2011, Monaco et al. 2011; macaques: Fattori et al. 2009, 2010, 2012). Other areas in the intraparietal sulcus process object size and shape during passive viewing, that is, irrespective of a pending grasping movement (macaques: Sereno and Maunsell 1998; Sereno et al. 2002; Sawamura et al. 2005; Lehky and Sereno 2007; humans: Sawamura et al. 2005; Konen and Kastner 2008; Monaco et al. 2010). Similarly, several human imaging studies have shown that the lateral occipital complex (LOC), a ventral stream area, is involved in processing object properties for grasping movements (Culham et al. 2003; Singhal et al. 2006; Monaco et al. 2010) as well as in viewing tasks (for reviews see Grill-Spector et al. 2001; Kourtzi and Connor 2011).

Given the well-established involvement of the dorsal stream in object-directed actions and the ventral stream in perception, it seems reasonable to assume that areas from both streams are involved in processing some aspects of object representation. However, while the role of ventral stream areas in object representation is well understood, the role of dorsal stream areas is less clear and more controversial. Some studies have shown that dorsal and ventral stream areas process object properties in fundamentally different ways, with dorsal stream areas processing action-dependent characteristics of images (such as viewpoint or orientation) and ventral stream areas processing object identity (James et al. 2002; Valyear et al. 2006; Cavina-Pratesi et al. 2007). In contrast, other studies found that both dorsal and ventral stream areas adapt to the similar features of objects, such as the viewpoint (Konen and Kastner 2008). This makes the interpretation of object representation in the dorsal stream quite controversial. Although some studies suggest that it reflects potential actions (Rice et al. 2007; Valyear et al. 2007), other studies attribute object representation in the dorsal stream to the integration of spatial and visual object properties despite action intention (Konen and Kastner 2008). In addition, although dorsal and ventral stream areas share the visual representation of object, the degree to which these areas are capable of discriminating between them is substantially

different, with the dorsal stream providing only a coarse representation of a shape, while the ventral stream exhibits a greater capacity in making finer shapes distinctions (Lehky and Sereno 2007; Srivastava et al. 2009).

One key aspect common to previous studies is that they manipulated extrinsic properties of objects (viewpoint or orientation) and intrinsic properties of objects (size or shape) without requiring any action, making it difficult to judge whether the processing of certain object features is indeed related to actions, such as grasping. In addition, it has not been addressed whether and which brain regions make a distinction between the coding of the specific graspable axis and the processing of global size or shape. The answers to these questions will help clarify some of the controversy about the role of brain areas involved in object representation and will shed light on the neural networks involved in the extraction of action-relevant information from general object properties.

Here, we address these questions using an functional magnetic resonance imaging (fMRA) adaptation design that independently manipulates size and grasp-relevant dimension of 3-dimensional (3D) objects in grasping and passive viewing tasks. In pairs of subsequent trials, we varied the grasp-relevant dimension of an object while keeping its size constant and vice versa. Therefore, the grasp-relevant dimension, object size, or both could either be repeated or novel. We hypothesized that cortical areas typically involved in grasping movements would show adaptation for the grasp-relevant dimension of an object, regardless of its size. We further conjectured that ventral stream areas typically involved in object representation would be modulated by global features, that is, object size, regardless of the potential graspable dimension. Our results show a more intricate picture, with adaptation to object size in calcarine and extrastriate visual areas regardless of the grasp-relevant dimension, an interaction between size and graspable dimension in the anterior intraparietal sulcus (aIPS), and finally adaptation to the grasp-relevant dimension regardless of size in the SPOC, lateral occipital complex (LOC), and dorsal premotor area (dPM). In addition, we find a visual-to-sensorimotor gradient from posterior to anterior regions, with larger adaptation to object size for viewing conditions in occipital areas and larger adaptation to the grasp-relevant dimension for grasping conditions in frontal areas, suggesting that motor processing was complete at this stage. Taken together, our results indicate a gradual processing from object size to object grasp-relevant dimension from posterior to anterior cortical areas and provide a complete cortical circuit for progressive transformation of general object properties into grasp-related responses.

Materials and Methods

Participants

Fourteen participants (6 males and 8 females, age range: 20–42 years) participated in this study and were financially compensated for their time. All participants were right-handed and had normal or corrected-to-normal visual acuity. They gave their consent prior the experiment. This study was approved by the York University Human Participants Review Subcommittee.

Experimental Design

We used an fMR adaptation paradigm (Grill-Spector et al. 1999) to investigate brain areas involved in processing the grasp-relevant dimension of an object during grasping and passive viewing tasks. In pairs of sequential events, a 3D real object was presented with either the same grasp-relevant dimension or different grasp-relevant dimensions and either in the same or different sizes (Fig. 1*A*). We had a combination of 2 tasks: Grasp (G) and View (V), 2 levels in the grasp-relevant dimension: Repeated (rD) and novel (nD), and 2 levels regarding object size: Repeated (rS) and novel (nS) that gave rise to a $2 \times 2 \times 2$ factorial design, which yielded 8 experimental conditions.

Participants were required either to use their dominant (right) hand to grasp the object or to passively view the object. At the beginning of each trial, participants received instructions about the task through a recorded voice that said "Grasp" or "View." At the end of each action, participants returned the hand to the starting position on the chest and kept it still in between trials. In the grasping conditions, participants grasped the object by opposing the index finger and the thumb as in a precision grip. The grasp-relevant dimension coincided with the bottom-up axis of the object, according to which the grip had to be scaled by using the same wrist posture in all trials. The grasp was performed without lifting the object. In the passive viewing conditions, participants were asked to attend the object without performing any action. In all conditions, participants were required to attend to the location of the object without moving their eyes from the fixation point. In summary, the critical difference between grasping conditions was that the grasp-relevant dimension, but not the size, required an appropriate adjustment of the grip aperture. Therefore, we hypothesized that brain areas involved in processing the critical grasping dimension would show adaptation for the repeated versus a novel grasp-relevant dimension regardless of size in grasping but viewing conditions.

Apparatus and Stimuli

Stimuli were presented to the participants on the inclined surface of a turntable placed above the participant's pelvis (Fig. 1*B*). Each participant lay supine in the scanner with the head tilted allowing a direct view of the stimuli without mirrors. Participants wore headphones to hear audio instructions about the task that they were to perform on the upcoming trial. Although the right forearm was free to move, the upper arm was strapped to the bed to be kept still. This helped to avoid artifacts due to the motion of the shoulder and the head (Culham et al. 2003).

The turntable was reached by the participant (from inside the bore) to perform the task and by the experimenter (from outside the bore) to change the stimulus in between trials. The turntable (radius = 40 cm) was mounted atop a platform, which was fixed to the bore bed through hooked feet. The turntable and the platform were made of Plexiglas. The location of the platform could be adjusted to ensure that both the participant and the experimenter could reach it comfortably. The head of the participant was tilted by 20° to allow comfortable viewing of the stimuli. The inclination of the platform could also be adjusted to improve the view and the reachability of the object for each participant. A divider mounted perpendicularly on the turntable prevented the participant from seeing the upcoming stimulus on the other side and the experimenter changing the stimulus. A rectangular surface was angled atop each half of the turntable to improve the visibility of the object (Fig. 1*B*). The objects were secured to the turntable through fitted pins, so that the location and the orientation of the objects were consistent across all trials. A lateral stopper on the platform prevented the turntable from being presented off-center with respect to the subject when the experimenter spun the turntable and prevented it from moving during participant's actions. A cloth was mounted on the ceiling of the magnet bore to occlude the participant's view of the experimenter.

For the experimental runs, the stimuli consisted of a cube (5 cm × 5 cm × 1.8 cm) and a cuboid (10 cm × 5 cm × 1.8 cm), shown in Figure 1*A*, made from Plexiglas and painted white to increase the contrast with the dark workspace. The angular size of the objects was approximately 4° for the small object and approximately 8° for the big object, and they were presented at approximately 10–12° of eccentricity in the lower periphery. Participants practiced the task and familiarized with the objects for about 5 min prior the experiment. For the independent functional localizer runs, we used 3D shapes

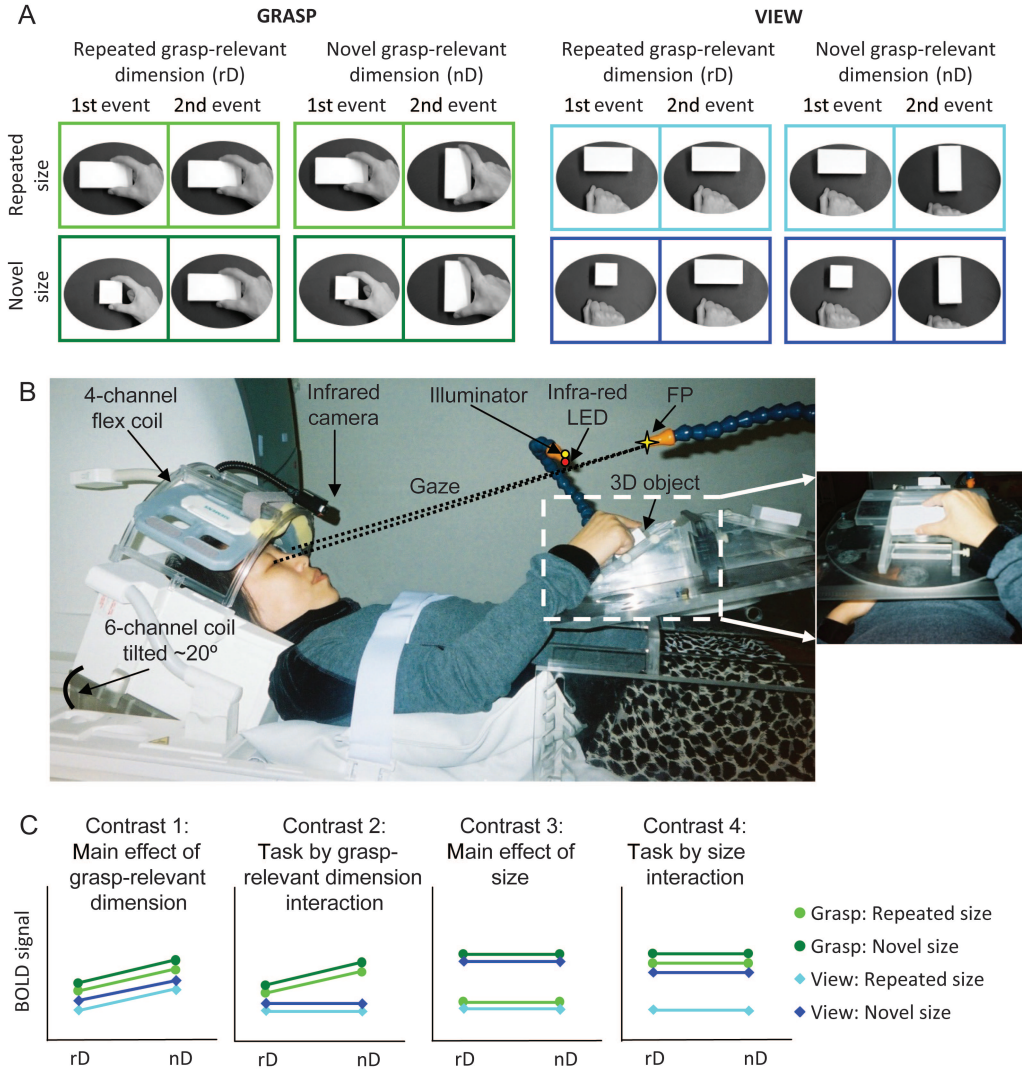

Figure 1. Schematic representation of the tasks and setup. (*A*) For each task (Grasp and View), each pair of sequential events involved 2 different object sizes (novel size), 2 different grasp-relevant dimensions (novel grasp-relevant dimension), or a repetition of one or both geometric properties (novel size, repeated grasp-relevant dimension; repeated size, novel grasp-relevant dimension; repeated size, repeated grasp-relevant dimension). In the grasping conditions, the object required different grip apertures when the grasp-relevant dimension was changing (right), but not necessarily when the size was changing (left). (*B*) The set-up required participants to gaze at the fixation point (FP, marked with a star), while performing the tasks. (*C*) Predicted changes in BOLD signal based on our 4 contrasts with the voxelwise group data for the experimental runs. We investigated the adaptation effects between novel and repeated conditions for grasping (green) and viewing (blue). We hypothesized that areas involved in processing the graspable dimension of objects would adapt to repeated grasp-relevant dimensions regardless of size as in contrast no. 1. Areas involved in processing the size of objects would adapt to repeated size regardless of the grasp-relevant dimension, as in contrast no. 3. We had no specific predictions regarding differences in adaptation effects between grasping and viewing conditions.

made from white plastic. They had a constant depth (1 cm), but varied in length (from 6 to 10 cm) and width (from 5 to 10 cm).

Except for the 2 sequentially illuminated presentations of the objects, subjects were in near-complete darkness throughout the duration of the trial (only a small dim light was provided by fixation). During the intertrial interval (ITI), and after the participant had performed the first event of the task, the object was quickly replaced and the turntable rotated by the experimenter even when the stimuli were repeated in the next trial to prevent participants from guessing the characteristics of the second object based on the perceived rotation of the board.

Optic fibers were used to provide a fixation point, to illuminate the workspace, and to cue the experimenter regarding stimuli on upcoming trials. The participant maintained the fixation on one point of light positioned approximately 10–15° of visual angle above the object, so that all objects were presented in the participant's lower visual field. A bright light (illuminator) was used to briefly illuminate the stimulus at the onset of each event of a trial. The illuminator was placed above the participant's head and shone light onto the object. Another source of light was based at the end of the platform, visible to the experimenter, but not to the participant, to instruct the experimenter about size and grasp-relevant dimension of the objects in the next 2 events. All of the lights and audios were controlled by a program in MatLab® 7.1 (The MathWorks, Inc., Natick, MA, USA) on a laptop PC that received a signal from the MRI scanner at the start of each trial. The windows in the scanner room were blocked and the room lights remained off such that, with the exception of the dim fixation point which remained on continuously, nothing else in the workspace was visible to the participant when the illuminator was off.

An infrared camera (MRC Systems GmbH) recorded the performance of each participant for offline investigation of the errors, which were excluded from further analysis. The errors were defined as mistakes in the performance of the participants during the task

(i.e. initiating a movement in the viewing condition, performing a reach in a grasp condition or vice versa). Less than 2% of total trials were discarded from the analyses due to participants' errors.

Timing and Experimental Conditions

We used a slow event-related design to prevent contamination of the blood oxygen level-dependent (BOLD) response by any potential artifacts generated by the hand movement. Trials were spaced every 16 s to allow the hemodynamic signal to return to baseline between trials. Each trial started with the audio cue instructing the participant about the task to be performed. After 2 s (from the onset of the audio cue), the first stimulus was illuminated for 250 ms, cueing the participant to perform the instructed task. The onsets of the first and second events were separated by 4 s, during which the experimenter rotated the turntable to position the second object for the next event. The brief illumination (250 ms) of the second object was the cue for the participant to perform the instructed task. Note that the brief periods of illumination ensured that the participants performed all the actions without visual feedback (in open loop).

Each run consisted of 32 trials and each experimental condition was repeated 4 times in a random order. A baseline of 18 s was added at the beginning and at the end of each run yielding a run time of approximately 13 min per run. Each of the 9 possible pairs of objects was evenly distributed through each run. Each participant performed 4 runs, for a total of 16 trials per experimental condition.

Independent Functional Localizer

In addition to the comparisons between experimental conditions, we also ran an independent functional localizer that allowed us to localize areas typically involved in reaching and grasping movements (Culham et al. 2003). In each trial, participants performed 1 of the 3 possible tasks (Grasp, Reach, or View) toward a briefly presented 3D stimulus. Unlike the experimental runs, each trial consisted only of a single presentation of a stimulus. Grasping and viewing tasks were similar to those in the experimental runs. In the reaching task, participants moved their closed hand toward the object to touch it with the knuckles.

We used a slow event-related design with one trial every 18 s to allow the hemodynamic response to return to baseline during the ITI. This localizer has been reliably used in several published studies over the past years to localize areas involved in grasping and reaching movements (Singhal et al. 2006; Cavina-Pratesi et al. 2007; Monaco et al. 2011). A given trial started with the auditory instruction of the task to be performed: "Grasp," "Reach," or "View." After 2 s from the onset of the audio cue, the stimulus was illuminated for 250 ms cuing the participant to initiate the task. Following the onset of the illumination was a 16-s interval to allow the hemodynamic response to return to baseline before the next trial began. Each localizer run consisted of 18 trials and each condition was repeated 6 times in a random order for a run time of approximately 7 min. Each participant performed 2 localizer runs for a total of 12 trials per condition.

Session Duration

A session for one participant included set-up time (~45 min), 6 functional runs and 1 anatomical scan, and took approximately 2.5 h to be completed. We did not conduct eye tracking during the scan because there are no MR-compatible eye trackers that can monitor gaze in the head-tilted configuration.

Imaging Parameters

All imaging was performed at York University (Toronto, ON, Canada) using a 3-T whole-body MRI system (Siemens Magnetom TIM Trio, Erlangen, Germany). The posterior half of a 12-channel receive-only head coil (6 channels) at the back of the head was used in conjunction with a 4-channel flex coil over the anterior part of the head (Fig. 1*B*). The anterior part of the 12-channel coil was removed to allow the participant to see the stimuli directly and comfortably but at a cost of anterior signal loss, hence the addition of the 4-channel flex coil. The posterior half of the 12-channel coil was tilted at an angle of 20° to allow the direct viewing of the stimuli. We used an optimized T_2-weighted single-shot gradient echo echo-planar imaging (211-mm field of view [FOV] with 64×64 matrix size, yielding a resolution of 3.3-mm isovoxel; 3.3-mm slice thickness with no gap; repetition time [TR] = 2 s; echo time [TE] = 30 ms; flip angle [FA] = 90°). Each volume comprised 38 slices angled at approximately 30° from axial (i.e., approximately parallel to the calcarine sulcus) to sample occipital, parietal, posterior temporal, and posterior/superior frontal cortices. The slices were collected in ascending and interleaved order. During each experimental session, a T_1-weighted anatomical reference volume was acquired along the repeated orientation as the functional images using a 3D acquisition sequence ($256 \times 240 \times 192$ FOV with the repeated matrix size yielding a resolution of 1-mm isovoxel, inversion time, TI = 900 ms, TR = 2300 ms, TE = 5.23 ms, FA = 9°). The coil configuration used allowed coverage of most part of the brain, except for the ventral part of the cerebellum.

Preprocessing

Data were analyzed using the Brain Voyager QX software (Brain Innovation 1.10, Maastricht, The Netherlands). Functional data were superimposed on anatomical brain images, aligned on the anterior commissure–posterior commissure line, and transformed into Talairach space (Talairach and Tournoux 1988). The first 2 volumes of each fMRI scan were discarded to allow for T_1 equilibration. Functional data were preprocessed with spatial smoothing (full-width at half-maximum = 8 mm) and temporal smoothing to remove frequencies below 2 cycles per run. Slice-time correction with a cubic spline interpolation algorithm was also performed. Functional data from each run were screened for motion or magnet artifacts with cine-loop animation to detect eventual abrupt movements of the head. In addition, we ensured that no obvious motion artifacts (e.g., rims of activation) were present in the activation maps from individual participants. Each functional run was motion corrected using a trilinear/sinc interpolation algorithm, such that each volume was aligned to the volume of the functional scan closest to the anatomical scan. The motion correction parameters of each run were also checked: Runs that showed abrupt head motion over 1 mm were discarded from further analyses. Data from one participant were discarded from the analyses for abrupt head movements over 1 mm.

Data Analyses

We performed 2 types of analyses. First, to investigate which brain areas are involved in our task, we conducted voxelwise analyses using the experimental runs. Second, because we had specific hypotheses about certain areas in the grasping network, we performed an analysis using a region of interest (ROI) approach in single subjects with the independent localizer runs.

For each participant, we used a general linear model (GLM) that included a predictor for each condition. Each predictor was derived from a rectangular wave function (2 s or 1 volume for the localizer runs; 6 s or 3 volumes for the experimental runs) convolved with a standard hemodynamic response function (HRF; Brain Voyager QX's default double-gamma HRF). Because the stimulus presentation and action execution components of the HRF overlapped considerably, we treated them together as one event. In the experimental runs, we chose the time window (6 s) to cover the 2 sequential presentations of the object and the corresponding actions, including both the outgoing and returning phase of the second action, which did not exceed 2 s. We also ensured that the convolved hemodynamic profile of the 6-s rectangular wave function closely matched the (2-event) time courses of the Grasp and Look conditions averaged together (to avoid any selection bias favoring one condition over another). Errors in performance were modeled as predictors of no interest. In addition, the 6 motion parameters were added as covariates.

Voxelwise Analyses

In the experimental runs, the group random effects (RFX) GLM included 8 predictors for each participant (Fig. 1*A*). Contrasts were

performed on %-transformed beta weights (β), therefore β values are scaled with respect to the mean signal level. This normalization allows to retain individual effect size difference across subjects better than Z-transformation. To test our hypotheses, we ran 4 contrasts on the group data, see Figure 1*C* for a schematic representation of the adaptation effects investigated with the voxelwise contrasts. First, we hypothesized that areas involved in processing the grasp-relevant dimension of objects would show adaptation for the repeated grasp-relevant dimension revealed by the contrast: [(G:nD:rS + G:nDnS + V:nD:rS + V:nD:nS) > (G:rD:rS + G:rD:nS + V:rD:rS + V:rD:nS)] (contrast no. 1). Second, to explore areas involved in processing the grasp-relevant dimension specifically for grasping, we looked for areas showing a task-by-grasp-relevant dimension interaction, with adaptation to repeated versus novel grasp-relevant dimension in grasping, but not in viewing conditions. This interaction would be revealed by the conjunction analyses: [(G:nD:rS + G:nD:nS − G:rD:rS − G:rD:nS) and (V:nD:rS + V:nD:nS + V:rD:rS + V:rD:nS)] (contrast no.2). Third, to explore areas involved in processing object size, we looked for a main effect of size using the contrast: [(V:nD:nS + V:rD:nS + G:nD:nS + G:rD:nS +) > (V:nD:rS + V:rD:rS + G:nD:rS + G:rD:rS)] (contrast no.3). Fourth, to explore areas involved in processing object size in viewing tasks, we searched for areas showing a task-by-size interaction reflected in adaptation to repeated versus novel size in viewing, but not in grasping conditions. This effect would be revealed by the conjunction analysis [(V:rD:nS + V:nD:nS − V:rD:rS − V:nD:rS)] and (G:rD:rS + G:rD:nS + G:nD:rS + G:nD:nS)] (contrast no.4). Activation maps for group voxelwise results are overlaid on the averaged anatomical MRI in which the T_1 weighted images from all participants have been combined to allow an unbiased overview of anatomical overlaps of the sulci across participants.

For each activation map generated by each of the 4 contrasts, we performed the cluster threshold correction (Forman et al. 1995) using the Brain Voyager's cluster-level statistical threshold estimator plug-in (Goebel et al. 2006). This algorithm uses Monte Carlo simulations (1000 iterations) to estimate the probability of a number of contiguous voxels being active purely due to chance while taking into consideration the average smoothness of the statistical maps. Because map smoothness varies with the contrast, different contrasts have different cluster thresholds. In cases in which activation foci did not survive the cluster threshold correction at an alpha-correction level of 0.05 (but a priori hypotheses and other contrasts suggested that the activation could very well be genuine), we indicated the regions with a star. This approach allows the rigor of correction for multiple comparisons to reduce type I errors, while also identifying areas that may be vulnerable to type II errors, which often go unacknowledged (Lieberman and Cunningham 2009). For each area, we extracted the β weights for each participant in each condition for further analysis. The minimum cluster sizes were estimated at 17 functional voxels for the first contrast, 45 functional voxels for the second contrast, and 90 functional voxels for the fourth contrast. The size of one functional voxel was 3 mm^3, while one anatomical voxel was 1 mm^3; therefore for each contrast, the total volume of the clusters was 459, 1215, and 2430 mm^3 or anatomical voxels.

For areas defined by voxelwise contrasts, where the data were not selected by independent localizers, the analysis of variance (ANOVA; see Statistical Analyses) and data graphs are based on nonindependent contrasts. We have opted to include these to show unequivocally the adaptation effects for the grasp-relevant dimension and to enable the reader to easily see the pattern of results, including effects that are independent of the selection criteria. Contrasts that are nonindependent are clearly indicated in square brackets.

ROI Analyses

For the independent functional localizer runs, each subject's GLM included 3 separate predictors: Grasp, Reach, and View. For each participant, we used these runs to independently identify 4 ROIs that are typically part of the reaching and grasping network: SPOC, LOC, dorsal premotor cortex (dPM), and aIPS. The aIPS and SPOC ROIs have been identified with analyses used in the previous literature. In particular, an aIPS ROI has been identified by a comparison of (Grasp > Reach), which has been typical in past studies of the region (Binkofski et al. 1998; Culham et al. 2003; Frey et al. 2005; Begliomini, Caria, et al. 2007; Begliomini, Wall, et al. 2007), while a SPOC ROI has been identified by a conjunction analysis of [(Grasp > Baseline) and (Reach > Baseline) and (View > Baseline)], which has been used in a recent study of the region (Monaco et al. 2010). The conjunction analyses used to identify SPOC, revealed another focus of activation consistently located in the LOC, at the intersection between the posterior end of the inferior temporal sulcus and the lateral occipital sulcus. Because of its characteristic anatomical location, we suggest that this area is part of the MT+/LOC complex (Dumoulin et al. 2000). Since this focus of activation has not been localized with an object or motion localizer, we cannot determine whether it is LOC or the visual motion area in the middle temporal gyrus (MT+). However, LOC and MT+ largely overlap even when localized separately (Kourtzi and Kanwisher 2001) given the functional similarities in processing 2-dimensional (2D) shapes. Therefore, it is possible that the area we find in the occipito-temporal region comprises both LOC and MT+. Finally, we identified dorsal premotor area (dPM) by using a contrast defined by a conjunction analysis of [(Grasp > View) and (Reach > View) and (View > Baseline)]. We used this conjunction analyses based on the functional properties of the area dPM described in previous studies showing 1) the strong involvement of dPM in grasping and reaching actions, 2) the higher activation for grasping and reaching compared with viewing tasks (Cavina-Pratesi et al. 2010; Monaco et al. 2011), and 3) neuronal responses modulated by object fixation even in the absence of any grasping movement (Raos et al. 2004).

ROIs were defined by using a voxelwise contrast in each individual (as can be seen in Figs 5*A*, 6*A* and 7*A*). First, we found the voxel with peak activation near the expected location of the ROI: superior end of the parietal occipital sulcus for SPOC; junction of inferior temporal sulcus and lateral occipital sulcus for LOC; T-junction of superior frontal and precentral sulci for dPM; and junction of intraparietal and postcentral sulci for aIPS. Then, thresholds for each subject were set to lower thresholds and a box-shaped ROI of 512 mm^3 (8 mm × 8 mm × 8 mm) centered around the peak voxel was selected to include the most active voxels. The goal of this approach was to obtain ROIs in anatomically appropriate locations and with comparable cluster sizes across participants and areas (Table 4). For each ROI from each participant, we extracted the event-related time course of the experimental runs and calculated the peak latency of the percent BOLD signal change (%BSC) averaged across the 8 conditions. The peak latency fell approximately 4–6 s after the second event of a trial, consistent with the hemodynamic response lag of the fMRI response (Cohen 1997; Dale and Buckner 1997). We used the %BSC at the peak response (1 volume) for further analysis. Subjects that did not show activation in the expected anatomical location were not included in the analyses of the area.

Statistical Analyses

For each area, we performed an ANOVA using SPSS with 2 (task)-by-2 (grasp-relvant dimensions)-by-2 (sizes) factors on either the β weights (voxelwise analyses) or the %BSC (ROI analyses). Where the interactions reached significance (dPM, aIPS, calcarine sulcus, and extrastriate cortex in the left hemisphere), post hoc contrasts were carried out. Since only 2 × 2 interactions reached significance, for each interaction we ran 4 groups of comparisons specified in Table 2. We used 1-tailed paired-sample *t*-tests with a Bonferroni correction for 4 comparisons ($P < 0.0125$). Because the predicted adaptation effects are unidirectional (novel > repeated but not repeated > novel), 1-tailed comparisons were performed. Statistical differences are indicated on line graphs for the 8 conditions. To further illustrate the differences graphically with appropriate error bars for the adaptation effects, for each area, we computed differences in activation between novel and repeated trials for the key conditions, along with the 98.75% confidence limits on those difference values, such that difference scores with error bars that do not include zero indicate that the difference between the 2 conditions was significant at $P < 0.05$, corrected; otherwise it is not. We described statistical effects that are significant at a corrected *P*-value, unless specified.

Results

First, we provide a general picture by describing the voxelwise results of the group data investigated with specific contrasts using the experimental runs. Second, we report the results of the ROI analyses for 4 areas included in the grasping network (SPOC, LOC, aIPS, and dPM) and localized through the targeted contrast using the independent functional runs in individual participants.

Voxelwise Analyses (Averaged Data)

To test our hypotheses, illustrated in Figure 1*C*, we performed 4 voxelwise contrasts on the group data. The contrasts were aimed at investigating brain areas showing: 1) adaptation to the repeated object grasp-relevant dimension in grasping and viewing conditions, 2) adaptation to the repeated grasp-relevant dimension in grasping, but not in viewing conditions, 3) adaptation to repeated object size in grasping and viewing conditions, and 4) adaptation to repeated object size in viewing, but not in grasping conditions. Both Talairach coordinates and number of voxels for each area are reported in Table 1. Statistical values of the post hoc *t*-tests for each area are reported in Table 2. Voxelwise results are plotted in Figs 2*B* and 3*B*. Effects that are nonindependent are clearly indicated in square brackets.

As shown in Figure 2*A* (left panel), the activation map for the main effect of grasp-relevant dimension (contrast no. 1) showed 2 areas in the left hemisphere: A dorsal one, located in the superior end of the parietal occipital sulcus (SPOC) and a ventral one, located in the LOC at the intersection of the ascending limb of both the inferior temporal sulcus and the lateral occipital sulcus. Because of its characteristic location, we suggest that this area corresponds to the LOC (MT+/LOC). The anatomical location of the observed LOC area is very close to the lateral occipital tactile-visual region (LOtv) described by Amedi et al. (2001). The area LOtv is a part of the larger LOC and is involved in processing visual and tactile exploration of objects (see Fig. 2*A*, left panel and Table 3 for comparison with previous studies). However, given that the ROI analyses showed a main effect of the grasp-relevant dimension in an area located in the anatomical vicinity of this voxelwise-defined area, we report results of LOC in the voxelwise section for completeness. The activation map showing adaptation to the repeated grasp-relevant dimension specifically for grasping actions (contrast no. 2) revealed one area in the frontal cortex of the left hemisphere, located at the junction between the superior precentral sulcus and the caudal end of the superior frontal sulcus (Fig. 2*A*, right panel). The area we found with this voxelwise contrast lies at the junction between the precentral sulcus and the caudal end of the superior frontal sulcus, which corresponds to the anatomical location of a premotor region involved in visuo-motor hand tasks (Amiez et al. 2006). We suggest that this area corresponds to dPM. Note that the foci of LOC and dPM did not survive the cluster threshold correction, as indicated by the stars.

Contrast no. 3 did not reveal any main effect of size (data not shown). The activation map showing adaptation to repeated object size in viewing, but not in grasping conditions (contrast no. 4) revealed 2 areas in the occipital lobe of the left hemisphere (Fig. 3*A*): A medial area located along the calcarine sulcus and a more lateral one located in the extrastriate cortex, in the vicinity of the lunate sulcus.

To further explore the data, we ran 2 additional contrasts to determine whether any brain area showed adaptation for: 1) The grasp-relevant dimension in viewing, but not in grasping conditions: [(V:nD:rS + V:nD:nS − V:rD:rS − V:rD:nS) and (+G:nD:rS + G:nD:nS + G:rD:rS + G:rD:nS)], and 2) object size for grasping, but not for viewing conditions: [(G:rD:nS + G:nD:nS − G:rD:rS − G:nD:rS) and (V:rD:rS + V:nD:rS + V:rD:nS + V:nD:nS)]. These contrasts did not reveal any significant adaptation effect.

Table 1
Voxelwise analyses. Talairach coordinates and number of voxels

Brain areas	Talairach coordinates			No. of voxels
	X	*y*	*Z*	
LH LOC	−54	−64	−12	550
LH SPOC	−16	−72	30	568
LH dPM	−28	−6	53	264
LH calcarine	−26	−67	11	758
LH extrastriate	−36	−78	10	447

Note: Area abbreviations as in figure legends.
LH: left hemisphere; RH: right hemisphere.

Table 2
Voxelwise analyses. Statistical values

Brain areas	Main effects ($P < 0.05$)			Interactions ($P < 0.05$)		Paired *t*-tests ($P < 0.0125$)			
	Task (G > V)	Grasp-relevant dimension (nD > rD)	Size (nS > rS)	T-by-D	T-by-S				
Contrast no. 1									
LH SPOC	**0.002**	[**0.011**]	0.527	0.201	0.257	—	—	—	—
LH LOC	**0.001**	[**0.008**]	0.617	0.602	0.472	—	—	—	—
						G:nD > G:rD	V:nD > V:rD	G:nD > L:nD	G:rD > L:rD
Contrast no. 2									
LH dPM	**0.001**	0.394	0.997	[**0.041**]	0.186	[**0.012**]	0.522	**0.001**	**0.001**
						G:nS > G:rS	V:nS > V:rS	G:nS > L:nS	G:rS > L:rS
Contrast no. 4									
LH calcarine	**0.003**	0.794	0.507	0.725	[**0.002**]	0.081	[**0.001**]	0.029	**0.001**
LH extrastriate	**0.018**	0.396	0.695	0.688	[**0.012**]	0.149	[**0.004**]	0.245	**0.001**

Note: Area abbreviations as in figure legends.
Significant values are indicated in boldface. Contrasts and values listed in square brackets are expected given the criteria used to select the region (i.e., nonindependent).
T: task; D: grasp-relevant dimension; S: size; G: grasp; V: view; n: novel; r: repeated.

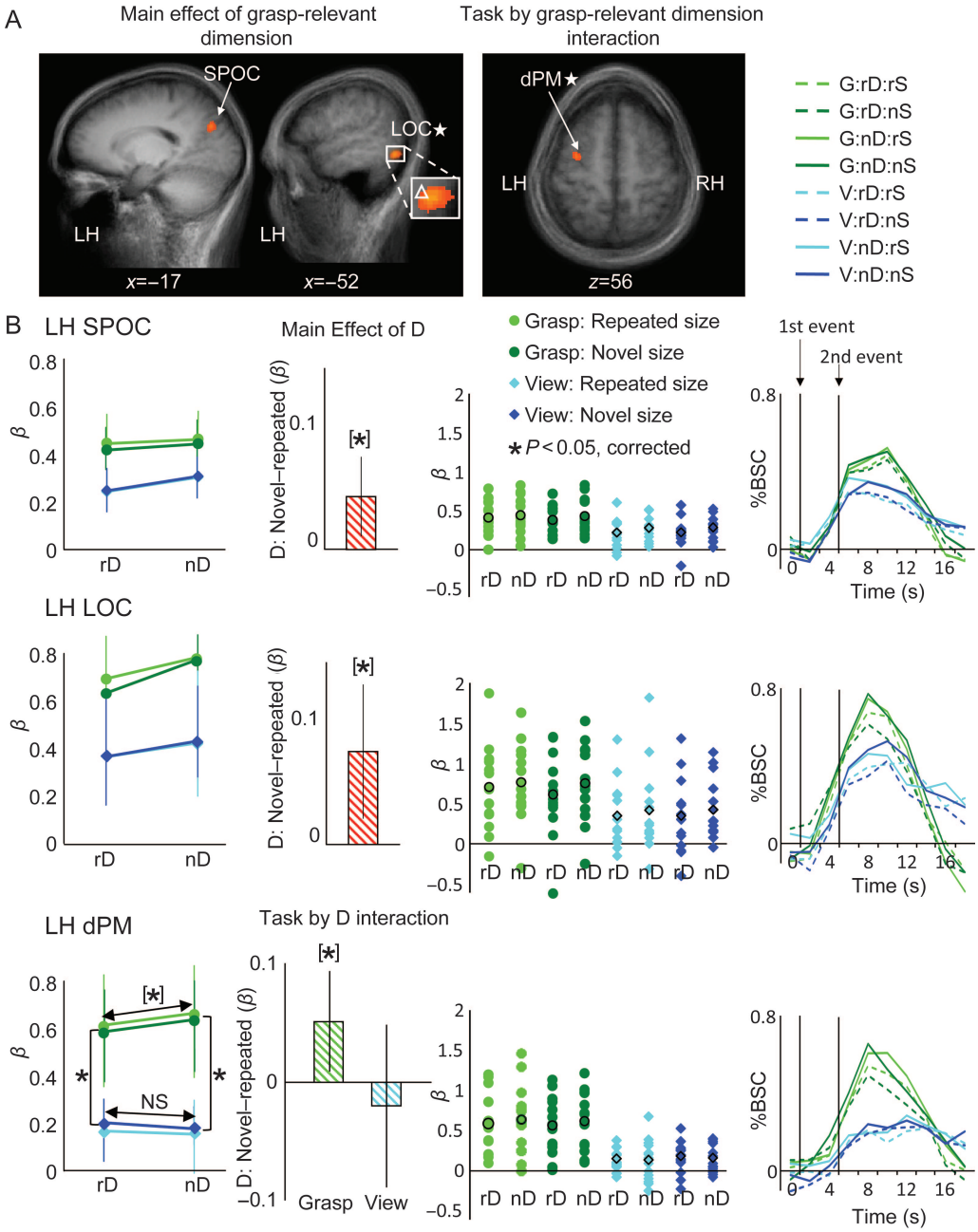

Figure 2. Voxelwise statistical maps obtained with the RFX GLM on the average anatomical MRI of all participants and activation levels for each area. (*A*, left panel) The map shows adaptation for repeated as opposed to the novel grasp-relevant dimension by using contrast no. 1 ($F > 2.4$, $k = 459$ mm^3). (Right panel) The map shows adaptation for repeated as opposed to the novel grasp-relevant dimension in grasping, but not in viewing conditions by using contrast no. 2 ($F > 2.4$, $k = 1215$ mm^3). White triangle in LOC indicates the average Talairach coordinates of area the lateral occipital tactile-visual region (LOtv) shown in other studies to allow a comparison. The stars beside LOC and dPM indicate that activation foci did not survive the cluster threshold correction for the contrasts used for the activation map. (*B*) For each area, line graphs (left) indicate the β weights for the 8 experimental conditions in the 3 areas, bar graphs show the difference in β weights between key conditions, scatter plots show the β weights for the 8 experimental conditions for each participant along with the average (black circles), time course graphs (right) show averaged %BSC. rD: repeated grasp-relevant dimension; nD: novel grasp-relevant dimension; rS: repeated size; nS: novel size. *Significant statistical differences among conditions for $P < 0.05$. [*] Significant effects that are nonindependent given the criteria used to select the region. NS: not significant. Error bars indicate 98.75% confidence intervals.

From Size to Grasp-Relevant Dimension: Posterior-to-Anterior Gradient

We investigated whether the processing of object size and grasp-relevant dimension followed a posterior to anterior gradient with decreasing adaptation to size in viewing conditions and with increasing adaptation to the grasp-relevant dimension in grasping conditions from occipital to frontal areas.

To this end, we performed a correlation analysis on adaptation effects calculated on Z-transformed beta weights (β). Therefore, the standard deviation of the BOLD signal was used for the normalization of Z-transformed data across different brain regions. We estimated the variation of the adaptation effects as a function of the location in the sagittal plane (*Y* Talairach coordinate) of each area in the left hemisphere

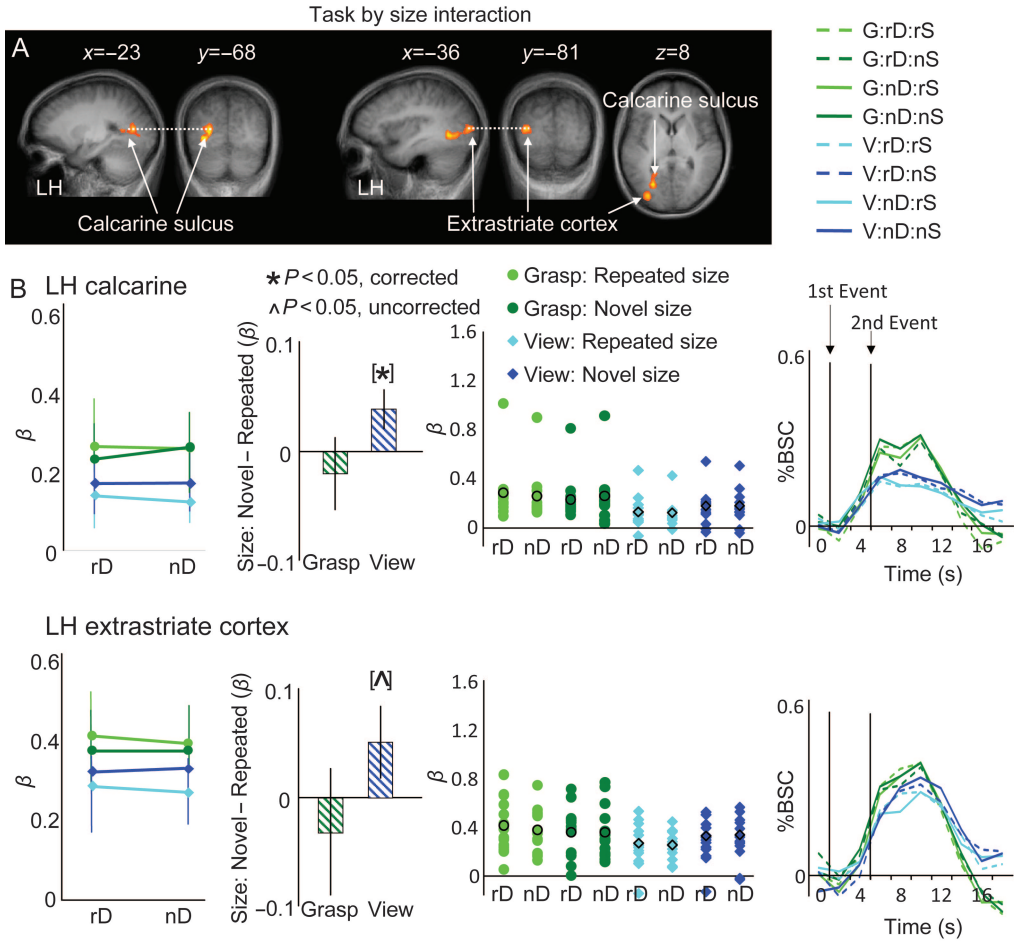

Figure 3. Voxelwise statistical maps obtained with the RFX GLM and activation levels for areas showing adaptation when viewing at objects with repeated as opposed to novel sizes. (*A*) The map shows a significant effect in the interaction by using the contrast no. 4 ($F > 2.4$, $k = 2430$ mm^3). (*B*) For each area, line graphs (left) indicate the β weights for the 8 experimental conditions in the 3 areas, bar graphs show the difference in β weights between key conditions, scatter plots show the β weights for the 8 experimental conditions for each participant along with the average (black circles), time course graphs (right) show averaged %BSC. ^ Statistical differences among conditions for $P < 0.05$, uncorrected. Other legends as in Figure 2.

Table 3
Summary of LOtv foci from other published papers and the present experiment

Publication	Area	Tal Coordinates		
		X	*Y*	*Z*
Amedi et al. (2001)	LHLOtv	−45	−62	−9
Amedi et al. (2002)	LHLOtv	−47	−62	−10
Amedi et al. (2007)	LHLOtv	−48	−59	−9
Tal and Amedi (2009)	LHLOtv	−48	−54	−8
Amedi et al. (2010)	LHLOtv	−41	−62	−6
Average LHLOtv		−45.8	−59.8	−8.4
		Voxelwise analyses		
Present results	LHLOC	−54	−64	−12
		ROI analyses		
Present results	LHLOC	−42	−60	−16

Note: List of studies reporting activation in the LOtv and relative locations expressed in Talairach coordinates.

revealed by the voxelwise analyses: Extrastriate cortex, calcarine sulcus, SPOC, LOC, and dPM. As shown in Figure 4, there was a positive correlation between sagittal coordinates and adaptation to the grasp-relevant dimension in grasping tasks ($R^2 = 0.98$), indicating progressive adaptation to grasp-related object properties from posterior to anterior brain regions. In contrast, there was a negative correlation between sagittal coordinates and adaptation to size in viewing tasks ($R^2 = 0.65$), indicating progressive decreasing adaptation to general object properties from posterior to anterior brain regions. In addition, there was no correlation between sagittal coordinates and adaptation to the grasp-relevant dimension in viewing tasks ($R^2 = 0.07$) and no correlation between sagittal coordinates and adaptation to size in grasping tasks ($R^2 < 0.01$).

To further examine the data, we ran an ANOVA on the adaptation effects with 5 (areas)-by-4 (adaptation to size for viewing, adaptation to size for grasping, adaptation to the grasp-relevant dimension for viewing, and adaptation to the grasp-relevant dimension for grasping) factors. In order to investigate differences among the 4 adaptation effects, we ran 2-tailed post hoc *t*-tests corrected for 6 comparisons ($P < 0.0083$). The ANOVA revealed a pattern of results consistent with the correlation analyses. Specifically, adaptation to size for viewing was larger than adaptation to the grasp-relevant dimension for grasping in the posterior (occipital) regions, while adaptation to the grasp-relevant dimension for grasping was larger than adaptation to size for viewing in the anterior (frontal) regions, and there was no preference to

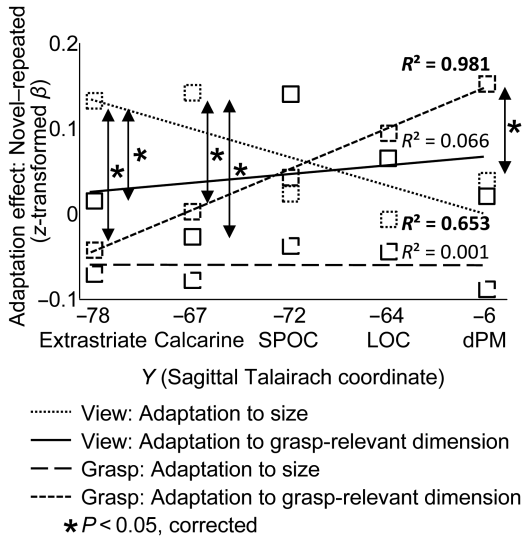

Figure 4. Correlation analysis between posterior-to-anterior location of brain areas in the left hemisphere and the adaptation effects to grasp-relevant dimension and size in viewing and grasping tasks. *Significant statistical differences among conditions indicated by the arrow for $P < 0.05$.

Table 4
ROI analyses. Talairach coordinates and number of voxels

Brain areas	Talairach coordinates			Average no. of voxels
	X	*Y*	*Z*	
LH SPOC	−49	−64	−3	513
LH LOC	−42	−60	−16	499
LH dPM	−26	−15	54	567
LH aIPS	−43	−37	43	500

Note: Talairach coordinates and numbers of voxels have been averaged across participants. Number of participants for each ROI: 14 for left SPOC and left LOC, 12 for left dPM, and 14 for left aIPS.
LH: left hemisphere.

either size or grasp-relevant dimension in the intermediate regions. There was a significant interaction ($F_{12,156} = 2.3$, $P < 0.05$), and post hoc *t*-tests showed that adaptation to size in viewing conditions was higher than that to the grasp-relevant dimension in grasping conditions in extrastriate cortex and calcarine sulcus (extrastriate: $t_{(13)} = 3.13$, $P < 0.05$; calcarine: $t_{(13)} = 3.24$, $P < 0.05$). In contrast, dPM showed the opposite pattern of results with a strong trend toward higher adaptation to grasp-relevant dimension in grasping conditions than to size in viewing conditions ($t_{(13)} = 1.74$, $P = 0.05$, uncorrected). In addition, extrastriate cortex and calcarine sulcus showed higher adaptation to size in viewing than in grasping conditions (extrastriate: $t_{(13)} = 3.19$, $P < 0.05$; calcarine: $t_{(13)} = 4.35$, $P < 0.005$). On the other hand, dPM showed higher adaptation to the grasp-relevant dimension in grasping than in viewing conditions ($t_{(13)} = 3.3$, $P < 0.05$).

ROI Analyses

The Talairach coordinates and numbers of voxels of each ROI are specified in Table 4.

SPOC and LOC

For the independent functional localizer runs, the conjunction analyses comparing each of the Grasp, Reach, and View conditions versus Baseline [i.e., (Grasp > Baseline) and (Reach > Baseline) and (View > Baseline)] revealed consistent activation in 2 regions: The first one was located at the superior end of the parieto-occipital sulcus (Fig. 5*A*, top panel), while the second one was located at the junction of the posterior end of the inferior temporal sulcus and the lateral occipital sulcus (Fig. 5*A*, bottom panel). We localized both SPOC and LOC in the left hemisphere of all 14 participants.

The experimental runs showed that SPOC and LOC adapted to the grasp-relevant dimension of objects regardless of size (Fig. 5*B*). In particular, we found a main effect of task (SPOC: $F_{1,13} = 8.2$, $P < 0.05$; LOC: $F_{1,13} = 17.39$, $P < 0.05$) and a main effect of grasp-relevant dimension (SPOC: $F_{1,13} = 11.12$, $P < 0.05$; LOC: $F_{1,13} = 37.42$, $P < 0.05$). Specifically, there was higher adaptation for repeated versus novel grasp-relevant dimension and higher response for grasping than for viewing conditions.

aIPS

For the independent functional localizer runs, the contrast of (Grasp > Reach) revealed consistent activation near the junction of the intraparietal sulcus and the inferior segment of the postcentral sulcus. In particular, we identified aIPS in the left hemisphere of all 14 participants (Fig. 6*A*).

For the experimental runs, left aIPS showed adaptation for repeated versus novel grasp-relevant dimension, but only for novel size conditions (Fig. 6*B*). Specifically, we found a main effect of task ($F_{1,13} = 41.8$, $P < 0.0001$) and a main effect of grasp-relevant dimension ($F_{1,13} = 5.66$, $P < 0.05$) as well as a significant size-by-grasp-relevant dimension interaction ($F_{1,13} = 4.87$, $P < 0.05$). As shown by the bar graph in Figure 6*B*, there was higher adaptation for repeated versus novel grasp-relevant dimension in the novel size ($t_{(13)} = 4.17$, $P < 0.05$), but not in the repeated size condition ($t_{(13)} = 0.833$, $P = 0.94$). Another way to consider the interaction is that there was higher adaptation for repeated versus novel size in the novel grasp-relevant dimension ($t_{(13)} = 2.5$, $P < 0.05$ uncorrected), but not in the repeated grasp-relevant dimension condition ($t_{(13)} = 0.327$, $P = 0.327$). Finally, there was higher response for grasping than for viewing conditions.

Dorsal Premotor Cortex

For the independent functional localizer runs, the conjunction analyses comparing the Grasp and Reach conditions versus View and the View condition versus Baseline [i.e., (Grasp > View) and (Reach > View) and (View > Baseline)] revealed consistent activation at the T-junction of the superior precentral sulcus and the caudal end of the superior frontal sulcus. For the 14 participants, we localized dPM in the left hemisphere of 12 participants (Fig. 7*A*).

For the experimental runs, we found patterns consistent with the voxelwise analysis, showing significant adaptation to the repeated grasp-relevant dimension for grasping, but not for viewing conditions (Fig. 7*B*). Specifically, we found a main effect of task ($F_{1,11} = 78.6$, $P < 0.0001$), a main effect of grasp-relevant dimension ($F_{1,11} = 78.6$, $P < 0.0001$), and a significant task-by-grasp-relevant dimension interaction ($F_{1,11} = 5.13$, $P < 0.05$). As shown by the bar graph in Figure 7*B*, there was higher adaptation for repeated versus novel grasp-relevant

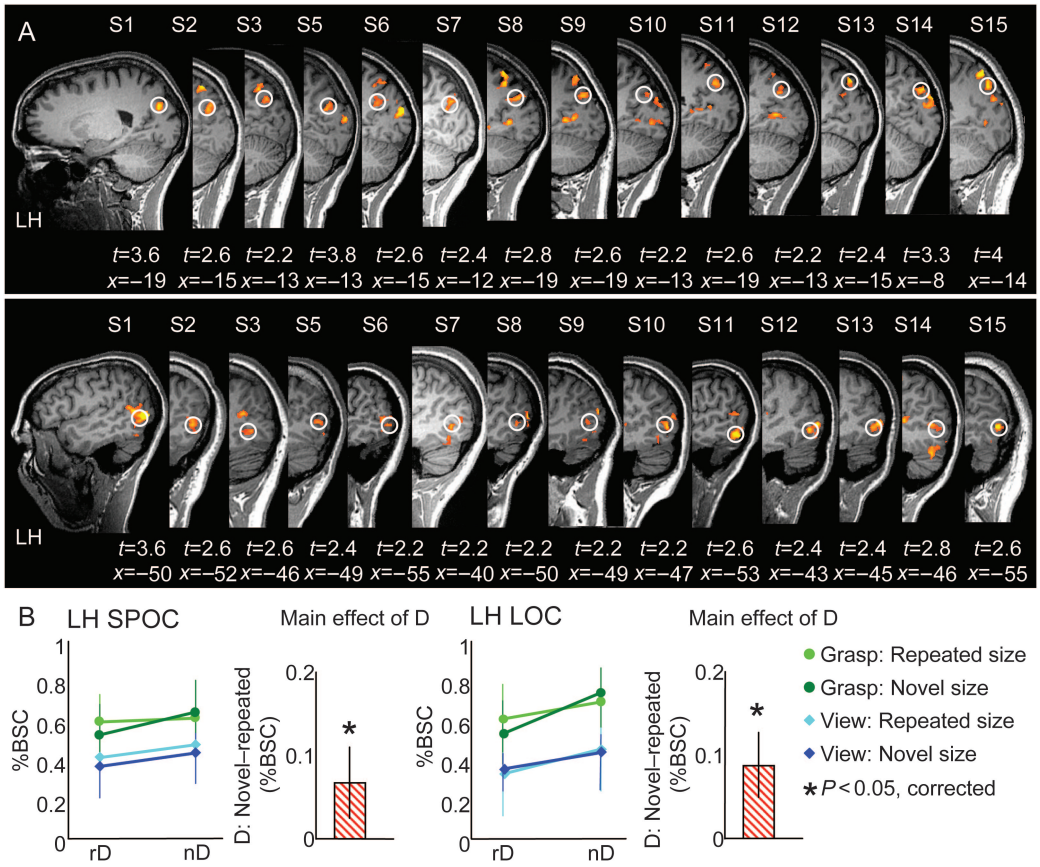

Figure 5. Individual statistical maps and activation levels across conditions for the superior parieto-occipital sulcus (SPOC) and LOC ROIs. (*A*) SPOC (upper panel) and LOC (lower panel) were identified in each participant with a conjunction analysis of [(Grasp > Baseline) and (Reach > Baseline) and (View > Baseline)] in independent functional localizer runs. We localized SPOC and LOC in the left hemisphere (LH) of 14 participants. The positions of the regions (circled areas) are shown in the sagittal slice for each participant. SPOC was identified in the vicinity of the parieto-occipital sulcus (POS), while the LOC was identified at the junction between the inferior temporal sulcus and the lateral occipital sulcus. (*B*) Line graphs display the average magnitude of peak activation (%BSC) in each experimental condition for SPOC (left plots) and LOC (right plots).

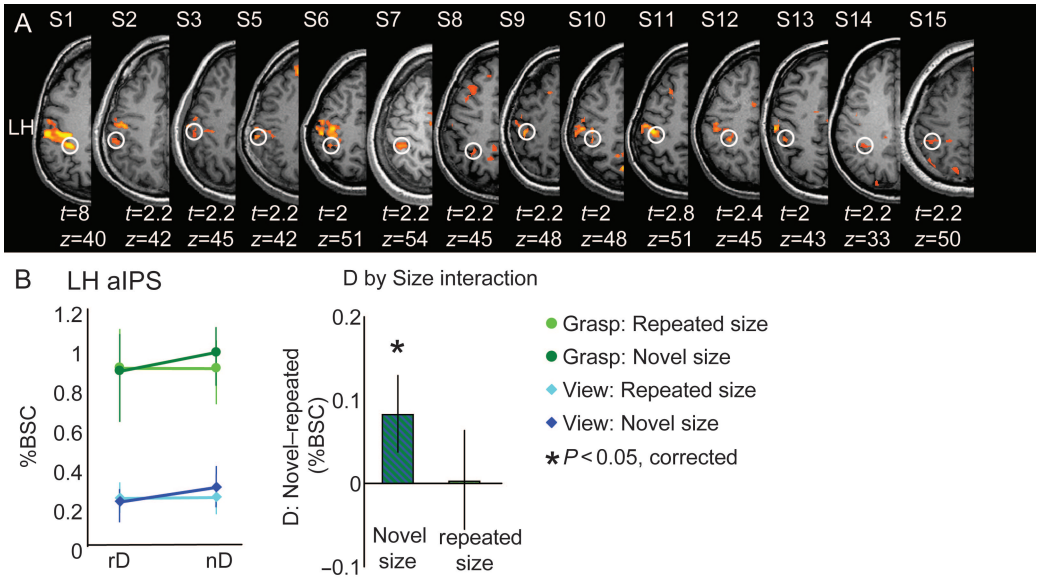

Figure 6. Individual statistical maps and activation levels across conditions for the aIPS ROI. (*A*) aIPS was identified in each participant with a contrast of (Grasp > Reach) in independent functional localizer runs. We localized aIPS in the left hemisphere of 14 participants. The position of the region (circled area) is shown in the transverse slice for each participant. The aIPS area was identified in the vicinity of the junction of the anterior end of the intraparietal sulcus and the inferior segment of the postcentral sulcus. (*B*) Line graphs display the average magnitude of peak activation (%BSC) in each experimental condition for the left aIPS. Bar graphs show the interaction by displaying the difference in peak activation (%BSC) between key conditions: "nS:nD – nS:rD and "rS:nD – rS:rD."

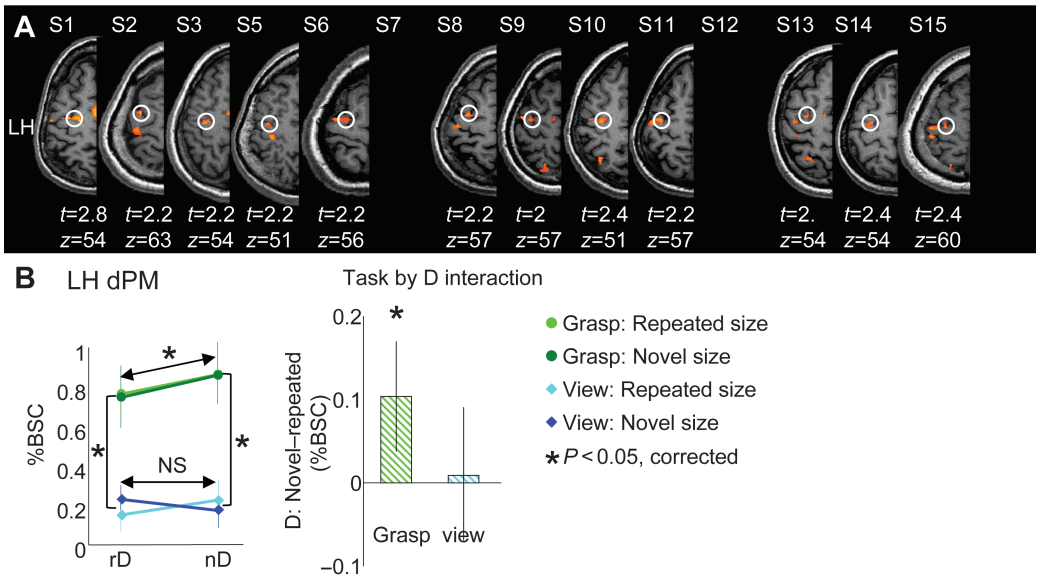

Figure 7. Individual statistical maps and activation levels across conditions for the dPM ROI. (*A*) dPM was identified in each participant with a conjunction analysis of [(Grasp > View) and (Reach > View) and (View > Baseline)] in independent functional localizer runs. We localized dPM in the left hemisphere of 12 of 14 participants. The position of the region (circled area) is shown in the transverse slice for each participant. The dPM region was identified in the vicinity of the junction of the superior frontal sulcus and the precentral sulcus. (*B*) Line graphs display the average magnitude of peak activation (%BSC) in each experimental condition for the left dPM. Bar graphs show the interaction by displaying the difference in peak activation (%BSC) between key conditions: "G:nD – G:rD" and "V:nD – V:rD."

dimension, but only in the Grasp condition ($t_{(11)} = 3.59$, $P < 0.05$). In contrast, there was no adaptation for repeated versus novel grasp-relevant dimension in the View condition ($t_{(11)} = 0.26$, $P = 0.4$). In addition, as shown by the line graph in Figure 7*B*, there was higher activation for Grasp versus View in the repeated grasp-relevant dimension ($t_{(11)} = 7.61$, $P < 0.05$) as well as in the novel grasp-relevant dimension condition ($t_{(11)} = 9.4$, $P < 0.05$).

Adaptation Effects in Visual Areas: Object Properties or Object Identity?

We performed *t*-tests between critical conditions in calcarine sulcus and LOC in the left hemisphere to rule out the possibility that the adaptation effects were driven by perceived changes in object identity as a consequence of variations in object properties, like orientation and length. This pattern would have been reflected in adaptation effects only when all object properties were repeated (as in the repeated grasp-relevant dimension: Repeated size condition), but not when any of the object properties was novel within a trial (as in the remaining 3 conditions). In fact, any change in object length or orientation would have led to a different object identity as opposed to the condition in which the same object was presented in subsequent events of a trial.

If object length and orientation had affected the perception of object identity leading to the observed adaptation effects in viewing conditions in V1, we would have found significant adaptation to size only in repeated, but not in novel grasp-relevant dimension conditions. However, pairwise *t*-tests revealed adaptation to size for viewing tasks in both repeated ($P < 0.05$) and novel grasp-relevant dimension ($P < 0.05$) conditions (Fig. 8, top panel). In addition, repeated size conditions elicited comparable responses in both repeated (mean BOLD signal: 0.14) and novel grasp-relevant dimension conditions (mean BOLD signal: 0.12), suggesting

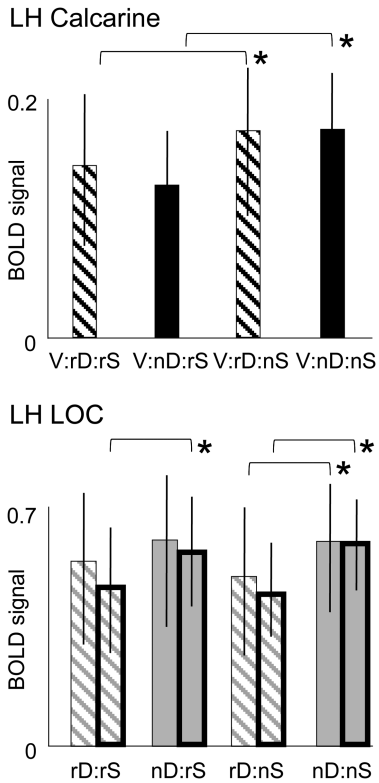

Figure 8. Activation levels and statistical comparisons between key conditions in calcarine sulcus and LOC to exclude adaptation to object identity. The BOLD signal from voxelwise (β weights) and ROI (%BSC) analysis is shown with thin and thick line bars, respectively. *Significant statistical differences among conditions for $P < 0.05$.

that object identity did not affect the response in the calcarine sulcus in a significant way.

Similarly, had object length and orientation affected the perception of object identity leading to the observed

adaptation effect in LOC, we would have found significant adaptation to the grasp-relevant dimension only in repeated, but not in novel size conditions. To explore this possibility, we ran pairwise *t*-tests on beta weights (β) and %BSC of area LOC defined with voxelwise and ROI analyses, and found that adaptation to the grasp-relevant dimension occurred in repeated ($P < 0.05$ for %BSC, $P = 0.07$ for β) as well as in novel size ($P < 0.05$ for %BSC and β) conditions (Fig. 8, lower panel). In addition, repeated grasp-relevant dimension conditions elicited comparable responses in repeated (mean BOLD signal: 0.47 for %BSC, 0.55 for β) as well as in novel size conditions (mean BOLD signal: 0.44 for %BSC, 0.5 for β), suggesting that object length (or size) did not affect the response in LOC in a significant way, unless it was relevant for grasping.

Discussion

Our results demonstrate 2 main findings. First, areas in the parietal-frontal network (SPOC and dPM), as well as a ventral stream area (LOC), are clearly involved in processing objects' grasp-relevant dimension rather than size. Second, we found a task-dependent effect in calcarine and extrastriate visual areas with adaptation to object size in viewing, but not in grasping conditions, and in dPM with adaptation to the grasp-relevant dimension for grasping, but not for viewing conditions. In contrast, intermediate parietal and lateral occipito-temporal areas show adaptation to the grasp-relevant dimension regardless of the task, revealing a more flexible and encompassing encoding across tasks.

Adaptation to Grasp-Relevant Dimension in SPOC, LOC, and aIPS

Our results show that SPOC and LOC process object's graspable dimension in grasping and viewing tasks. The fact that SPOC and LOC belong to the dorsal and ventral stream, respectively, might lead to the expectation that these 2 areas code object properties in a fundamentally different way, with SPOC processing properties that are directly related to action (i.e., graspable dimension), while LOC processing holistic representations of objects (i.e., size). In contrast, our results show that these 2 areas process common characteristics of objects. Importantly, adaptation to the graspable dimension in SPOC and LOC occurred for both grasping and viewing tasks, suggesting that the effects are not only an epiphenomenon of sensorimotor feedback. The processing of grasp-relevant dimension for passive viewing reflects the potential for action evoked by the object (Gibson 1979) even when the action is not explicitly planned. These results are consistent with studies providing evidence for the coding of intention in the parietal cortex (macaques: Snyder et al. 1997, 2000; Scherberger and Andersen 2007; humans: Gallivan et al. 2011) and action recognition (Shmuelof and Zohary 2005). Our results show that this coding mechanism extends to a ventral stream area (LOC), suggesting that posterior parietal cortex and occipital temporal cortex might work in concert to extract grasp-relevant dimensions from overall object properties for potential actions. Several neuroimaging studies have shown the involvement of SPOC and LOC in grasping actions (Culham et al. 2003; Cavina-Pratesi et al. 2007, 2010; Kroliczak et al. 2008; Gallivan et al. 2011). A study using transcranial magnetic stimulation has demonstrated that while disruptions to the parietal cortex lead to impairments in both online and delayed control of grasping, lesions to LOC lead to the impairment only of delayed grasping (Cohen et al. 2009). Regardless of whether the impairment occurs for immediate or delayed actions, these results are evidence of a clear involvement of both areas in processing object features relevant for grasping. The fact that there was higher activation for grasping than for viewing tasks suggests that the observed effects are not due only to vision of the object, and that action execution requires additional computations in these areas when compared with passive viewing alone.

The LOC showing adaptation to the graspable dimension might represent only a subdivision of the bigger LOC. Indeed, the anatomical location of this area is very close to LOtv described by Amedi et al. (2001). Activation in LOC has been found in grasping tasks to visually explored objects (Culham et al. 2003; Cavina-Pratesi et al. 2007, 2010; Monaco et al. 2010) and hand movement tasks solely based on somatosensory input (Fiehler et al. 2008). In light of the present results, we speculate that the lateral occipital complex might code the association between intrinsic visual properties of objects and their relation with the somatosensory experience of grasping, for which the graspable dimension would be the crucial feature of the object.

Our results in aIPS show a unique pattern of adaptation suggesting an integration of information about graspable dimension and object size. Neurophysiology studies have shown that macaque AIP neurons are modulated by intrinsic visual properties of objects (such as the size), and that some neuronal activity showed a precise correspondence between preferred object and preferred grip (Murata et al. 2000). Our results show that the activation for processing grasp-relevant dimensions of objects is enhanced when both this dimension and overall object size are being coded. Anatomical and neuroimaging studies have shown that aIPS is connected with other posterior parietal regions, frontal premotor areas, and inferotemporal cortex (macaques: Borra et al. 2008; Gamberini et al. 2009; humans: Verhagen et al. 2008). These studies suggest that aIPS represents a node for converging information about objects' features (through connections with the ventral areas) and motor-relevant object cues for movement planning and execution (through connections with the posterior parietal and frontal areas). Another possibility is that the adaptation effects to grasp-relevant dimensions in the aIPS varied as a function of object shape rather than object size. In fact, it is likely that, in our design, changes in object size were also perceived as changes in shape, leading to adaptation in aIPS, a region shown to adapt to object shape for grasping movements in humans (Kroliczak et al. 2008) as well as in primates (Murata et al. 2000). Regardless of whether aIPS showed sensitivity to object size or shape, our results highlight the crucial role of aIPS in complementing sensory-motor information for grasping with global features for object representation.

Unlike previous fMRI studies that have shown adaptation to object size in the LOC (Grill-Spector et al. 1999; Sawamura et al. 2005), we did not observe adaptation to size with our stimuli. Null results in fMRA are difficult to interpret, particularly in areas like LOC, which codes multiple categories and dimensions of images of objects, but has failed to show adaptation to real 3D objects (Snow et al. 2011). Therefore, differences in results might be due to methodological differences: While Sawamura, Grill-Spector and colleagues used 2D stimuli

(Grill-Spector et al. 1999; Sawamura et al. 2005), here we employed real 3D objects. Difference in results due to the employment of different stimuli would not be surprising considering that different neural mechanisms are involved in processing 2D versus real 3D stimuli. For example, a recent fMRA study has shown that the neural processing involved in the perception of real-world 3D objects is fundamentally distinct from that for 2D planar representation of the same items, and that this difference is likely attributable to additional depth cues provided by binocular vision or the physical presence of the objects for 3D, but not for 2D objects (Snow et al. 2011). Our results in the LOC are in agreement with an fMRI study showing the involvement of LOC in a size discrimination task, in which real 3D stimuli differed in the size by variations of the grasp-relevant dimension (Cavina-Pratesi et al. 2007). Similar reasons can be used to explain the absence of adaptation to object size in parietal areas. Previous studies have shown the coding of object size in the intraparietal sulcus using 2D (Sawamura et al. 2005; Konen and Kastner 2008) as well as 3D stimuli (Monaco et al. 2010), but changes in object size also lead to changes in the grasp-relevant dimension, and thus these 2 features could not be dissociated from each other.

Adaptation to Grasp-Relevant Dimension for Grasping in dPM

Our results suggest a crucial role of dPM in coding the parameters of an object that are critical for the execution of a grasp, suggesting a motor-related processing of object features. Our findings are consistent with evidence that dPM neurons are sensitive to the grasp type required by different objects (Stark et al. 2007) and corroborate the "motor representation" interpretation put forward by Raos et al. (2004). This interpretation suggests that dPM has a representation of objects in motor terms, and it is based on evidence that neurons in macaque area dPM show congruent responses for the most effective grip and the presentation of objects that require that particular grip. In humans, the preparatory activity in dPM can be used to decode grasping movements toward a big or a small cube several seconds before action execution (Gallivan et al. 2011). Our results show that the discrimination between different object sizes in dPM is strictly related to the graspable dimension of the object rather than to its size, and that this processing extends to the execution phase of the movement. The present finding suggests different possible scenarios about the role of this area: First, dPM might be involved in the visuomotor representations of actions. Specifically, it might process the hand posture required by an object with a specific grasp-relevant dimension, disregarding the global features of the object, such as its size. Second, it is possible that the observed adaptation effect reflects the sensorimotor feedback necessary for the control of grasping movements. Indeed, different graspable dimension would require different adjustments of distal muscle for scaling the proper fingers posture. Regardless of whether the fMRA reflects the required hand posture or the sensory-motor control during the action, dPM is clearly implicated in analytical processing of objects dimension specifically related to the action.

Adaptation to Size for Viewing in Occipital Areas

This study is the first to demonstrate adaptation to 3D object size in V1. In particular, our effects were localized above the posterior end of calcarine sulcus in the left hemisphere, consistent with the fact that objects were presented in the lower visual field. This result suggests that early visual areas might be involved in processing global object features, in fact the object size changed for the 2 objects presented sequentially in novel, but not in repeated size conditions. Remarkably, the adaptation effects in early visual areas were specifically related to the size of the object, rather than to object identity. In fact, adaptation effects to object size were present in repeated as well as in novel grasp-relevant dimension conditions, suggesting that changes in object orientation or length that might have contributed to the perception of different object identity did not play a significant role in the observed pattern of results.

The fact that the adaptation effect was detected only in the left hemisphere might indicate that the processing of general object properties was stronger in the hemisphere contralateral to the hand used to perform the action. These results suggest that the adaptation effects to size and grasp-relevant dimension are part of a network in which object properties are processed for the ultimate goal of extracting information for action. Although the visual system is traditionally known to be organized in early visual areas (i.e., V1, V2, V3, and V4) involved in the analyses of local features (Hubel and Wiesel 1968) and in higher visual areas (i.e., the occipito-temporal cortex) involved in processing global shapes (Felleman and Van Essen 1991; Van Essen et al. 1992; for review: Maunsell and Newsome 1987), there is growing evidence that early visual areas are also involved in processing global visual configurations (Allman et al. 1985; Gilbert 1992, 1998; Lamme et al. 1998; Fitzpatrick 2000; Kourtzi et al. 2003; for reviews, Kapadia et al. 1995, 1999; Zipser et al. 1996; Polat et al. 1998). In particular, Kourtzi et al. (2003) have shown selective adaptation to global features in peripheral V1, corresponding anatomically to the calcarine sulcus.

Progressive Transformation of Object Properties: From Perceiving An Object to Executing An Action

Our results reveal the presence of a posterior to anterior gradient with a preference for object size in viewing conditions in the occipital lobe and with a preference for the grasp-relevant dimension in grasping conditions in the frontal lobe. This gradient suggests that object properties are represented in progression across posterior to anterior networks. This progression is related to the task and object properties and shows that while occipital and frontal areas are highly specialized in processing one object property over the other in a task-specific manner, parietal and lateral occipito-temporal cortices appear to be less task-specialized, emphasizing the associative functions of these areas. These results are consistent with the idea that objects are processed differently depending on the task. A behavioral study by Ganel and Goodale (2003) has shown that when planning and executing a grasp, people analytically process the graspable dimension of an object by isolating it from the nongraspable dimensions. However, in a perceptual task, the judgment of one dimension is affected by other dimensions of the object. Our results support and extend these findings by showing that this behavioral difference is reflected in the pattern of activity in different brain areas.

Conclusions

Our results show evidence that adaptation to object properties in both the dorsal and ventral stream areas is closely related to the analysis of action-relevant features of objects rather than object representation per se. These results reinforce the suggestion that the 2 visual streams work in concert for the production of skillful actions. Further studies are needed to investigate the role of dorsal and ventral stream areas in the integration of visual and spatial information of real 3D objects for perception and action.

To conclude, our results provide a complete cortical circuit for the progressive transformation of general object properties in posterior occipital areas into grasp-related responses more anteriorly in lateral occipital, parietal, and frontal areas. This transformation can be explained by the fact that overall object properties that are initially processed and perceived through visual areas (calcarine and extrastriate visual areas) are then filtered by parietal and lateral occipital areas (SPOC, LOC, and aIPS), which integrate visual information about the object with possible motor outputs, restricting the analyses of the object to those features that are most relevant for possible actions. Once the processing of the motor output is complete, frontal areas (dPM) process specific object properties that are relevant for the task being planned and executed.

Funding

This work was supported by the Natural Sciences and Engineering Research Council of Canada to D.Y.P.H. and the TransCoop-Program from the Alexander von Humboldt Foundation assigned to D.Y.P.H. and K.F., D.Y.P.H. is an Alfred P. Sloan fellow. W.P.M. is supported by a starting grant from the European Research Council. S.M. is supported by the NSERC CREATE CAN-ACT program.

Notes

We thank Joy M. Williams for help during data collection, Edgar Ghahramanyan for help with programming the experiment, Jody C. Culham and Patrick A. Byrne for helpful advice regarding data analyses, and Liana Brown for insightful discussion about the paradigm. *Conflict of Interest*: None declared.

References

Allman J, Miezin F, McGuinness E. 1985. Stimulus specific responses from beyond the classical receptive field: neurophysiological mechanisms for local-global comparisons in visual neurons. Annu Rev Neurosci. 8:407–430.

Amedi A, Jacobson G, Hendler T, Malach R, Zohary E. 2002. Convergence of visual and tactile shape processing in the human lateral occipital complex. Cereb Cortex. 12(11):1202–1212.

Amedi A, Malach R, Hendler T, Peled S, Zohary E. 2001. Visuo-haptic object-related activation in the ventral visual pathway. Nat Neurosci. 4(3):324–330.

Amedi A, Raz N, Azulay H, Malach R, Zohary E. 2010. Cortical activity during tactile exploration of objects in blind and sighted humans. Restor Neurol Neurosci. 28(2):143–156.

Amedi A, Stern WM, Camprodon JA, Bermpohl F, Merabet L, Rotman S, Hemond C, Meijer P, Pascual-Leone A. 2007. Shape conveyed by visual-to-auditory sensory substitution activates the lateral occipital complex. Nat Neurosci. 10(6):687–689.

Amiez C, Kostopoulos P, Champod AS, Petrides M. 2006. Local morphology predicts functional organization of the dorsal premotor region in the human brain. J Neurosci. 26(10):2724–2731.

Asher I, Stark E, Abeles M, Prut Y. 2007. Comparison of direction and object selectivity of local field potentials and single units in macaque posterior parietal cortex during prehension. J Neurophysiol. 97(5):3684–3695.

Begliomini C, Caria A, Grodd W, Castiello U. 2007. Comparing natural and constrained movements: new insights into the visuomotor control of grasping. PLoS One. 2(10):e1108.

Begliomini C, Wall MB, Smith AT, Castiello U. 2007. Differential cortical activity for precision and whole-hand visually guided grasping in humans. Eur J Neurosci. 25(4):1245–1252.

Binkofski F, Dohle C, Posse S, Stephan KM, Hefter H, Seitz RJ, Freund HJ. 1998. Human anterior intraparietal area subserves prehension: a combined lesion and functional MRI activation study. Neurology. 50(5):1253–1259.

Borra E, Belmalih A, Calzavara R, Gerbella M, Murata A, Rozzi S, Luppino G. 2008. Cortical connections of the macaque anterior intraparietal (AIP) area. Cereb Cortex. 18(5):1094–1111.

Cavina-Pratesi C, Goodale MA, Culham JC. 2007. FMRI reveals a dissociation between grasping and perceiving the size of real 3D objects. PLoS One. 2(5):e424.

Cavina-Pratesi C, Monaco S, Fattori P, Galletti C, McAdam TD, Quinlan DJ, Goodale MA, Culham JC. 2010. Functional magnetic resonance imaging reveals the neural substrates of arm transport and grip formation in reach-to-grasp actions in humans. J Neurosci. 30(31):10306–10323.

Chouinard PA, Large ME, Chang EC, Goodale MA. 2009. Dissociable neural mechanisms for determining the perceived heaviness of objects and the predicted weight of objects during lifting: an fMRI investigation of the size-weight illusion. Neuroimage. 44(1):200–212.

Cohen MS. 1997. Parametric analysis of fMRI data using linear systems methods. Neuroimage. 6(2):93–103.

Cohen NR, Cross ES, Tunik E, Grafton ST, Culham JC. 2009. Ventral and dorsal stream contributions to the online control of immediate and delayed grasping: a TMS approach. Neuropsychologia. 47 (6):1553–1562.

Culham JC, Danckert SL, DeSouza JF, Gati JS, Menon RS, Goodale MA. 2003. Visually guided grasping produces fMRI activation in dorsal but not ventral stream brain areas. Exp Brain Res. 153 (2):180–189.

Dale AM, Buckner RL. 1997. Selective averaging of rapidly presented individual trials using fMRI. Hum Brain Mapp. 5(5):329–340.

Dumoulin SO, Bittar RG, Kabani NJ, Baker CL Jr, Le Goualher G, Bruce Pike G, Evans AC. 2000. A new anatomical landmark for reliable identification of human area V5/MT: A quantitative analysis of sulcal patterning. Cereb Cortex 10(5):454–463.

Fattori P, Breveglieri R, Raos V, Bosco A, Galletti C. 2012. Vision for action in the macaque medial posterior parietal cortex. J Neurosci. 32(9):3221–3234.

Fattori P, Breveglieri R, Marzocchi N, Filippini D, Bosco A, Galletti C. 2009. Hand orientation during reach-to-grasp movements modulates neuronal activity in the medial posterior parietal area V6A. J Neurosci 29(6):1928–1936.

Fattori P, Raos V, Breveglieri R, Bosco A, Marzocchi N, Galletti C. 2010. The dorsomedial pathway is not just for reaching: grasping neurons in the medial parieto-occipital cortex of the macaque monkey. J Neurosci 30(1):342–349.

Felleman DJ, Van Essen DC. 1991. Distributed hierarchical processing in the primate cerebral cortex. Cereb Cortex. 1(1):1–47.

Fiehler K, Burke M, Engel A, Bien S, Rosler F. 2008. Kinesthetic working memory and action control within the dorsal stream. Cereb Cortex. 18(2):243–253.

Fitzpatrick D. 2000. Seeing beyond the receptive field in primary visual cortex. Curr Opin Neurobiol. 10(4):438–443.

Forman SD, Cohen JD, Fitzgerald M, Eddy WF, Mintun MA, Noll DC. 1995. Improved assessment of significant activation in functional magnetic resonance imaging (fMRI): use of a cluster-size threshold. Magn Reson Med. 33(5):636–647.

Frey SH, Vinton D, Norlund R, Grafton ST. 2005. Cortical topography of human anterior intraparietal cortex active during visually guided grasping. Brain Res Cogn Brain Res. 23(2–3):397–405.

Gallivan JP, McLean DA, Valyear KF, Pettypiece CE, Culham JC. 2011. Decoding action intentions from preparatory brain activity in human parieto-frontal networks. J Neurosci. 31(26):9599–9610.

Gamberini M, Passarelli L, Fattori P, Zucchelli M, Bakola S, Luppino G, Galletti C. 2009. Cortical connections of the visuomotor parietooccipital area V6Ad of the macaque monkey. J Comp Neurol. 513(6):622–642.
Ganel T, Goodale MA. 2003. Visual control of action but not perception requires analytical processing of object shape. Nature. 426 (6967):664–667.
Gardner EP, Babu KS, Ghosh S, Sherwood A, Chen J. 2007. Neurophysiology of prehension. III. Representation of object features in posterior parietal cortex of the macaque monkey. J Neurophysiol. 98(6):3708–3730.
Gibson JJ. 1979. The ecological approach to visual perception. Michigan: Houghton Mifflin. p. 332.
Gilbert CD. 1998. Adult cortical dynamics. Physiol Rev. 78(2):467–485.
Gilbert CD. 1992. Horizontal integration and cortical dynamics. Neuron. 9(1):1–13.
Goebel R, Esposito F, Formisano E. 2006. Analysis of functional image analysis contest (FIAC) data with brainvoyager QX: from single-subject to cortically aligned group general linear model analysis and self-organizing group independent component analysis. Hum Brain Mapp. 27(5):392–401.
Grill-Spector K, Kourtzi Z, Kanwisher N. 2001. The lateral occipital complex and its role in object recognition. Vis Res. 41(10–11):1409–1422.
Grill-Spector K, Kushnir T, Edelman S, Avidan G, Itzchak Y, Malach R. 1999. Differential processing of objects under various viewing conditions in the human lateral occipital complex. Neuron. 24(1):187–203.
Hubel DH, Wiesel TN. 1968. Receptive fields and functional architecture of monkey striate cortex. J Physiol. 195:215–243.
James TW, Humphrey GK, Gati JS, Menon RS, Goodale MA. 2002. Differential effects of viewpoint on object-driven activation in dorsal and ventral streams. Neuron. 35(4):793–801.
Kapadia MK, Ito M, Gilbert CD, Westheimer G. 1995. Improvement in visual sensitivity by changes in local context: parallel studies in human observers and in V1 of alert monkeys. Neuron. 15(4):843–856.
Kapadia MK, Westheimer G, Gilbert CD. 1999. Dynamics of spatial summation in primary visual cortex of alert monkeys. Proc Natl Acad Sci USA. 96(21):12073–12078.
Konen CS, Kastner S. 2008. Two hierarchically organized neural systems for object information in human visual cortex. Nat Neurosci. 11(2):224–231.
Kourtzi Z, Connor CE. 2011. Neural representations for object perception: structure, category, and adaptive coding. Annu Rev Neurosci. 34:45–67.
Kourtzi Z, Kanwisher N. 2001. Representation of perceived object shape by the human lateral occipital complex. Science. 293 (5534):1506–1509.
Kourtzi Z, Tolias AS, Altmann CF, Augath M, Logothetis NK. 2003. Integration of local features into global shapes: monkey and human FMRI studies. Neuron. 37(2):333–346.
Kroliczak G, McAdam TD, Quinlan DJ, Culham JC. 2008. The human dorsal stream adapts to real actions and 3D shape processing: a functional magnetic resonance imaging study. J Neurophysiol. 100 (5):2627–2639.
Lamme VA, Super H, Spekreijse H. 1998. Feedforward, horizontal, and feedback processing in the visual cortex. Curr Opin Neurobiol. 8(4):529–535.
Lehky SR, Sereno AB. 2007. Comparison of shape encoding in primate dorsal and ventral visual pathways. J Neurophysiol. 97 (1):307–319.
Lieberman MD, Cunningham WA. 2009. Type I and type II error concerns in fMRI research: re-balancing the scale. Soc Cogn Affect Neurosci. 4(4):423–428.
Maunsell JHR, Newsome WT. 1987. Visual processing in monkey extrastriate cortex. Annu Rev Neurosci. 10:363–401.
Monaco S, Cavina-Pratesi C, Sedda A, Fattori P, Galletti C, Culham JC. 2011. Functional magnetic resonance adaptation reveals the involvement of the dorsomedial stream in hand orientation for grasping. J Neurophysiol. 106(5):2248–2263.
Monaco S, Sedda A, Cavina-Pratesi C, Culham JC. 2010. Where is it? How big is it? Different brain areas answer different questions about graspable three-dimensional object properties in an fMRI adaptation experiment. Society for Neuroscience, San Diego, CA. Abstract. 893.3.
Murata A, Gallese V, Luppino G, Kaseda M, Sakata H. 2000. Selectivity for the shape, size, and orientation of objects for grasping in neurons of monkey parietal area AIP. J Neurophysiol. 83(5):2580–2601.
Polat U, Mizobe K, Pettet MW, Kasamatsu T, Norcia AM. 1998. Collinear stimuli regulate visual responses depending on cell's contrast threshold. Nature. 391(6667):580–584.
Raos V, Umilta MA, Gallese V, Fogassi L. 2004. Functional properties of grasping-related neurons in the dorsal premotor area F2 of the macaque monkey. J Neurophysiol. 92(4):1990–2002.
Rice NJ, Valyear KF, Goodale MA, Milner AD, Culham JC. 2007. Orientation sensitivity to graspable objects: an fMRI adaptation study. Neuroimage. 36(Suppl 2):T87–T93.
Sawamura H, Georgieva S, Vogels R, Vanduffel W, Orban GA. 2005. Using functional magnetic resonance imaging to assess adaptation and size invariance of shape processing by humans and monkeys. J Neurosci. 25(17):4294–4306.
Scherberger H, Andersen RA. 2007. Target selection signals for arm reaching in the posterior parietal cortex. J Neurosci. 27 (8):2001–2012.
Sereno AB, Maunsell JH. 1998. Shape selectivity in primate lateral intraparietal cortex. Nature. 395(6701):500–503.
Sereno ME, Trinath T, Augath M, Logothetis NK. 2002. Three-dimensional shape representation in monkey cortex. Neuron. 33 (4):635–652.
Shmuelof L, Zohary E. 2005. Dissociation between ventral and dorsal fMRI activation during object and action recognition. Neuron. 47 (3):457–470.
Singhal A, Kaufman L, Valyear K, Culham JC. 2006. fMRI reactivation of the human lateral occipital complex during delayed actions to remembered objects. Vis Cogn. 14(1):122–125.
Snow JC, Pettypiece CE, McAdam TD, McLean AD, Stroman PW, Goodale MA, Culham JC. 2011. Bringing the real world into the fMRI scanner: repetition effects for pictures versus real objects. Sci Rep. 1:130.
Snyder LH, Batista AP, Andersen RA. 1997. Coding of intention in the posterior parietal cortex. Nature. 386(6621):167–170.
Snyder LH, Batista AP, Andersen RA. 2000. Intention-related activity in the posterior parietal cortex: a review. Vis Res. 40(10–12):1433–1441.
Srivastava S, Orban GA, De Maziere PA, Janssen P. 2009. A distinct representation of three-dimensional shape in macaque anterior intraparietal area: fast, metric, and coarse. J Neurosci. 29 (34):10613–10626.
Stark E, Asher I, Abeles M. 2007. Encoding of reach and grasp by single neurons in premotor cortex is independent of recording site. J Neurophysiol. 97(5):3351–3364.
Tal N, Amedi A. 2009. Multisensory visual-tactile object related network in humans: insights gained using a novel crossmodal adaptation approach. Exp Brain Res. 198(2–3):165–182.
Talairach J, Tournoux P. 1988. Co-planar stereotaxic atlas of the human brain. New York: Thieme Medical.
Valyear KF, Cavina-Pratesi C, Stiglick AJ, Culham JC. 2007. Does tool-related fMRI activity within the intraparietal sulcus reflect the plan to grasp? Neuroimage. 36(Suppl 2):T94–T108.
Valyear KF, Culham JC, Sharif N, Westwood D, Goodale MA. 2006. A double dissociation between sensitivity to changes in object identity and object orientation in the ventral and dorsal visual streams: a human fMRI study. Neuropsychologia. 44 (2):218–228.
Van Essen DC, Anderson CH, Felleman DJ. 1992. Information processing in the primate visual system: an integrated systems perspective. Science. 255(5043):419–423.
Verhagen L, Dijkerman HC, Grol MJ, Toni I. 2008. Perceptuo-motor interactions during prehension movements. J Neurosci. 28 (18):4726–4735.
Zipser K, Lamme VA, Schiller PH. 1996. Contextual modulation in primary visual cortex. J Neurosci. 16(22):7376–7389.